MSUCL-251
August 1977

FINE STRUCTURE IN THE GIANT RESONANCE REGION AND THE COLLECTIVE DIPOLE SPIN-FLIP EXCITATION IN ^{208}Pb

H.P.Morsch*, P.Decowski**, and W.Benenson
Cyclotron Laboratory, Michigan State University
E.Lansing, MI 48824

NUCLEAR REACTIONS $^{208}Pb(p,p')$, E=40 and 45 MeV, measured $\sigma(\theta)$; $^{208}Pb(\alpha,\alpha')$, E=48 MeV. Deduced excitation strengths for J=1,2 and 3 transitions in the excitation region 6-12 MeV.

Inelastic scattering of 40 and 45 MeV protons has been used to study the excitation region of 6-12 MeV in ^{208}Pb. This region is found to be strongly structured with states of different multipolarity. Fine structure peaks between 8.5 and 10 MeV show mainly quadrupole and octupole structure. The "Giant" M1 excitations observed recently are strongly excited and are described by microscopic form factors. Several strongly excited states between 6 and 8.5 MeV show angular distributions of characteristic dipole (L=1) structure. Ground state widths derived from our inelastic cross sections are many times larger than measured in γ induced reactions, this indicates a structure different from isovector dipole. These states may represent a collective dipole spin-flip excitation (L=1, S=1) which in a simple collective picture can be interpreted as a collective dipole oscillation of spin-up particles against spin-down particles. Two of these states at 7.40 and 7.92 MeV were identified in 180° electron scattering as 2^- states. Derived B(M2) values from our data are in excellent agreement with the electron scattering results. The other two states at 6.26 and 8.37 MeV may represent collective 1^- spin-flip excitations.

*Present address: Kernfysisch Versneller Instituut, Universiteit Groningen, Netherlands.

**Present address: Institute of Experimental Physics, University of Warsaw, Warsaw, Poland.

I. Introduction

In the study of nuclear excitations strong collective motion is of particular interest. Apart from the well-known giant dipole resonance (L=1,T=1) and the more recently observed giant quadrupole resonance, there are several other possible collective excitations which have not been established experimentally, e.g. the giant monopole resonance. There are also other types of dipole excitations, e.g. magnetic dipole (1^+) and dipole spin-flip, which are of considerable interest. Magnetic dipole excitations have been subject of extensive studies for ^{208}Pb where, except for $2\hbar\omega$ excitations, only the $h_{11/2}$ proton and the $i_{13/2}$ neutron spin-flip is possible. Two M1 excitations have been established recently [1,2] which yield a large portion of the M1 strength. In order to study collective modes in ^{208}Pb, we have measured inelastic proton scattering at 40 and 45 MeV with high resolution. We find that the low energy part of the giant resonance region is strongly structured and shows an angle dependence that indicates different multipolarity for the various fine structure peaks. Microscopic DWBA calculations are presented in which different collective model or shell model transition densities are folded into effective nucleon-nucleon interactions. Good fits to the measured angular distributions are obtained, and in most cases this determines the multipolarity of the transition. For a quantitative comparison with γ induced reactions an attempt is made to derive electromagnetic matrix elements and widths from our excitation strength.

II. Experiments and Results

The experiments were performed with protons from the Michigan State University Cyclotron. The scattered particles were detected in a delay line gas counter[3] on the focal plane of an Enge split pole spectrograph. Time of flight information from a plastic scintillator was used to eliminate slit scattered particles. Targets were prepared by deposition in vacuum of ^{208}Pb enriched to 99.1% onto 20 mg/cm^2 ^{12}C foil. For targets of $\approx$ 1 mg/cm^2 a resolution of 20 keV could be achieved and this was limited by the focal plane detector and beam resolution. Non-linearities of the detector and uncertainties in the background substraction lead to an error in the quoted excitation energies of 20 keV. By using a closed vacuum transport system the oxygen contamination was kept so low in the spectra that no peaks due to oxygen were observable. A spectrum is shown in Fig.1. Most data at 45 MeV, however, were taken using a target of 5.4 mg/cm^2 thickness which limited the resolution to about 35 keV. Angular distributions of the different states are given in Figs.3-7. Similar to the analysis in ref. 4, a local background of the type shown by solid and dashed lines in Fig. 1 was assumed. The angular distribution of the background has a monotonic fall-off to larger angles which decreases between 10° and 30° by 25-30%. In order to get more information on the structure of strong dipole excitations which we find at around 8 MeV, we measured inelastic α scattering with the same setup at an energy of 48 MeV. A spectrum of this reaction is shown in Fig. 8.

III. Microscopic Calculations

DWBA calculations were performed using microscopic form factors in which a real nucleon-nucleon interaction was folded into the transition density of the target nucleus.

A Serber force of Gaussian form of 1.68 fm range was used with a volume integral of the spin- and isospin-independent interaction of 446 MeV fm^3. This interaction yields a description of low-lying excitations in ^{208}Pb in excellent agreement with electromagnetic transition rates[5] and originates from potentials which fit few nucleon systems[6]. A few calculations have been performed with a Yukawa interaction of 1 fm range, by using a strength of 26 MeV one obtains quite similar differential cross sections as by using the Gaussian form above. This Yukawa interaction is consistent with the systematics of Austin[7]. The effective interaction was folded with microscopic and collective model transition densities. Microscopic densities were obtained by using single-particle radial wave functions generated in Woods-Saxon potentials with the geometry r_o=1.2 fm and a=0.65 fm. The well depth was adjusted to fit experimental binding energies. For multipolarities L=2 and 3, collective model transition densities were used which were a radial derivative of the ground state density. For dipole excitations, transition densities from Goldhaber-Teller[8] and Jensen-Steinwedel[9] models were used. The optical model parameters in the entrance and exit channels were taken from Becchetti and Greenlees' work[10]. Small changes of these parameters had little effect on the calculated angular distributions.

In the transition between initial $|i\rangle$ and final $|f\rangle$ states the inelastic form factor can be expressed by

$$\langle f|V_L^{ST}(r)|i\rangle=(2L+1)^{\frac{1}{2}}\,4\pi V_L^{ST}\int\rho_{TR}^{M}(r')g_L(r,r')r'^2dr' \qquad (1)$$

and the electromagnetic matrix element by

$$\langle f|O(EL)|i\rangle=(2L+1)^{\frac{1}{2}}\int\rho_{TR}^{C}(r')r'^{L+2}dr' \qquad (2)$$

where $\rho_{TR}^{M}(r')$ and $\rho_{TR}^{C}(r')$ are mass and charge transition density, respectively, and $4\pi V_L^{ST} \cdot g_L(r,r')$ is the L^{th} element in the multipole expansion of the nucleon-nucleon interaction $V^{ST}(r-r')=4\pi \sum_{L,M} V_L^{ST} g_L(r,r') Y_L^M(\theta,\phi) Y_L^{M*}(\theta',\phi')$

The transition density may be given by

$$\rho_{TR}^{M,C}(r') = \sum_{(M,C)}^{k} a_{fk}\, a_{ik}\, M_k\, u_{fk}(r')\, u_{ik}(r') \qquad (3)$$

where a_{ik} and a_{fk} are nuclear amplitudes and $u_{ik}(r')$ and $u_{fk}(r')$ the radial wave functions in the initial and final state, M_k are angular momentum coupling matrix elements[11]. In the sum k runs over all proton and neutron components for $\rho_{TR}^{M}(r')$ and over all charged particle components for $\rho_{TR}^{C}(r')$, respectively.

Simpler expressions are obtained if collective transition densities are used, in form of a simple surface derivative $\rho_{TR}(r')=\beta_L R \frac{\partial \rho(r')}{\partial r'}$ for transitions of multipolarity $L \geq 2$, or from Jensen-Steinwedel[9] or Goldhaber-Teller[8] model for L=1. If proton and neutron densities ρ_p and ρ_n are also assumed to be related by $\rho_n = \frac{N}{Z}\rho_p$ (in an isoscalar non-spin-flip mode) then a fixed relation between inelastic formfactor and electromagnetic matrix element is obtained in which $\rho_{TR}^{M}(r')= \frac{A}{Z}\rho_{TR}^{C}(r')$.
Also for the isovector dipole excitation the inelastic excitation is directly related to the B(E1) by the use of effective charges $\frac{N}{A}e$ and $-\frac{Z}{A}e$ for protons and neutrons, respectively.
The transition probability for electromagnetic transitions from a 0^+ ground state is given by

$$B(EL,\ i\to f) = e^2 |\langle f|O(EL)|i\rangle|^2$$

Because of the close relation of inelastic form factors and electromagnetic matrix elements energy weighted sum rules[12] for $r^L Y_L$ and $r^L Y_L \tau$ operators may be utilized to estimate collective strength in inelastic scattering. Using an effective charge of $\frac{Z}{A}e$ the isoscalar sum rule for multipolarity 2 or larger is given by

$$\sum_c |\langle f_c|O(EL)|i\rangle|^2 E_c = L(2L+1)^2 \frac{\hbar^2}{8\pi m} \frac{Z^2}{A} \langle r^{2L-2}\rangle_{g.s.} \qquad (4)$$

c sums over all states with excitation energy E_c. For monopole excitations the sum rule has the form

$$\sum_c |\langle f_c|r^2|i\rangle|^2 E_c = \frac{2\hbar^2}{m} \frac{Z^2}{A} \langle r^2\rangle_{g.s.} \qquad (5)$$

For isovector excitations the sum rule is more model dependent
By neglecting exchange terms the electric dipole operator with effective charges $\frac{N}{A}e$ and $-\frac{Z}{A}e$ for protons and neutrons, respectively, yields

$$\sum_c |\langle f_c|O(E1)|i\rangle|^2 E_c = \frac{9\hbar^2}{8\pi m} \frac{NZ}{A} \qquad (6)$$

Dipole spin flip excitations(L=1,S=1) may be described in analogy to the isovect dipole excitations as a movement of spin-up particles against spin-down particles and protons in phase (T=0) or out of phase (T=1) with the neutrons. This dipole spin-flip excitation mode can lead to spins of 0^-, 1^-, and 2^-; the 1^- and 2^- excitations correspond to E1 and M2, respectively, whereas the 0^- is not excited electromagnetically. The latter is strongly inhibited by the selection rules $j'=j$; $\ell'=\ell+1$.

To derive matrix elements for these transitions one may use, similar to the electric dipole operator $rY_1\tau$, operators in the form $r[Y_\lambda\sigma]^{\lambda=0-2}$ and $r[Y_\lambda\sigma]\cdot\tau^{\lambda=0-2}$ for isoscalar and isovector excitations, respectively. This yields expressions similar to that in eq. (2). The strength is given in units of e^2fm^2, the same as for the B(E1) transition rate. For 2^- excitations the B(M2) strength usually is given in units of $(\frac{\hbar}{2mc})^2.e^2fm^2; (\frac{\hbar}{2mc})^2 = 0.011\ fm^2$.

A rough estimate of the energy of this dipole spin-flip excitation may be given by the unperturbed energy $\hbar\omega$ plus the spin orbit splitting which in ^{208}Pb is in the order of 1 MeV for the low ℓ orbit and a few MeV for the high ℓ orbits. It should be noted that in this spin-flip mode protons are very differently excited than neutrons; in proton scattering the interaction is $V_\sigma = V_{0\sigma} + V_{1\sigma}$, with positive sign for protons and negative sign for neutrons. So for a Serber force (in which $V_{0\sigma} = V_{1\sigma}$) the proton-proton interaction is $2V_{0\sigma}$ and the proton-neutron interaction vanishes. However, the nuclear tensor force, which can be important in spin-flip excitations, may cause neutron excitation also.

In fig. 2 differential cross sections are shown for different collective excitation modes assuming an excitation of 100% of the energy weighted sum rules at an excitation energy of 10 MeV. For the dipole spin-flip the same sum rule strength is used as for the isovector dipole excitation. Very distinct differences are observed for different L transfer, and this can be utilized to determine the L value of the transitions. Coulomb-nuclear interference is important in the forward

angle region and this leads to a destructive interference for isoscalar non-spin-flip excitations, for which the nuclear interaction is attractive. For the isovector non-spin-flip excitation the Coulomb nuclear interference is constructive due to the repulsive nuclear interaction. The largest forward angle cross sections are obtained for the isovector dipole excitation. At our energies it is mainly due to Coulomb excitation and shows a very strong energy dependence.

IV. Discussion

The high energy resolution spectrum in fig. 1 shows a very rich structure in the high excitation region of ^{208}Pb. We concentrate on three subjects, fine structures in the region of the giant quadrupole resonance, the discussion of M1 excitations, and the recently observed[4] group of L=1 excitations in the energy region around 8 MeV. The latter is discussed in connection with isovector dipole transitions excited in proton scattering. In the high energy region we observed essentially quadrupole and octupole structure whereas below 8.5 MeV we find a large number of peaks which have rather featureless angular distributions with a slight increase towards larger angles indicating excitations of higher multipolarity. Overlapping structures of different multipolarity also yield unspecific angular distribution Therefore only strong structures with pronounced angular dependence could be unambiguously identified.

IV.1. Fine structure in the High Excitation Region 8.5 - 12 MeV

Our proton spectra show a pronounced structure in the high excitation region of ^{208}Pb. We observe many narrow peaks on the low-energy side of the giant quadrupole resonance. Angular distributions of many of the fine structure peaks are shown in fig.3. These are superimposed on a background which originates from compound and precompound reactions as well as giant resonance excitation. Except for a monopole excitation at 9.11 MeV which has been discussed in ref.4 we find only states of quadrupole and octupole character. DWBA calculations for L=2 and 3 isoscalar excitations are given in fig.3 along with the data. The sum rule strengths are given in table 1.

In addition to the fine structure peaks there is indication for gross structures (width of 300 keV or more) at 9.3, 10.1 and 11.1 MeV; there angular distributions are shown in fig.4. Except for the structure at about 9.3 MeV which is very pronounced in (p,p') (see also ref.13) the other structures are rather weak. This is very different from electron scattering[14,15] where pronounced structures are observed at around 10.1, 10.6 and 11.2 MeV. In ^{3}He scattering[4] and α scattering[16] the 9.3 MeV structure is observed but no clear evidence for the other structures is found. These differences in the excitation of gross structures in electron and hadron scattering are of large interest and may give insight into the character of these excitations. The fact that the high excitations (above 10 MeV) are weakly excited in (p,p') may indicate isovector excitation which is inhibited in proton scattering as compared to isoscalar excitation. To some extend this could explain also the less structured angular distributions in fig.4 observed for these structures: if in addition to T=0 excitations T=1 components contribute then less structured forward angle cross sections are obtained. This is shown by the 10.1 and 11.1 MeV structures in fig.4 where in addition to isoscalar excitations (L=3, 10% EWSR and L=2, 6% EWSR) isovector contributions (L=2, 0.5% and 1% sum rule) have been

assumed. Larger T=1 excitations are expected in the underlying resonance structure. It is monotonically falling towards larger angles; if only isoscalar excitation would be present then the background would be expected to be smaller in the region 10°-20°. The 9.3 MeV gross structure is seen equally strong in (p,p') and (^{3}He,^{3}He')[4] indicating a dominant isoscalar excitation. Its angular distribution is described by a sum of L=2 and 3 consistent with other results[4,13].

Another gross structure is observed in electron scattering at 8.9 MeV[14,15]. For this structure a monopole assignment has been made by ref.17. We observe in this region many fine structure peaks of quadrupole and octupole character which indicates mixed multipolarity in this region. A strong monopole excitation as proposed by ref.17 (50% of the sum rule strength) clearly can be ruled out. The fact that in the high resolution experiment of ref.18 less fine structure and a larger sum rule strength (35% EWSR (E2)) is observed as compared to our experiment may indicate additional isovector excitation.

The largest cross sections in fig.2 are obtained for the isovector dipole excitation which is almost entirely due to Coulomb excitation. Although in the (γ,n) reaction[19] quite strong dipole excitations are seen in the energy region in question little evidence for these excitations is found in our (p,p') spectra. Only the forward rise of the angular distribution for the 9.38 MeV state may indicate the strong dipole transition at about 9.42 MeV seen in ref.19.

IV.2. Magnetic Dipole (1^{+}) Excitations

Magnetic dipole excitations in ^{208}Pb are of particular interest because they involve (in addition to possible admixtures of 2ħω particle-hole excitations) only the $h_{11/2}$ proton and the $i_{13/2}$ neutron spin-flip components. As discussed above, in these spin-flip transitions the $i_{13/2}$ neutron componen is not excited in proton scattering (if a nuclear force of Serber type is assumed). The present experimental situation on these excitations is as follo

above the neutron threshold one strong M1 state at 8.00 MeV has been identified by Holt and Jackson in a neutron polarization experiment[1]. Below the neutron threshold a second M1 excitation has been recently found at 7.06 MeV[2]. In the present proton scattering experiment rather strong states at 8.01 and 7.06 MeV are observed. Although the corresponding angular distributions (shown in fig.5) are too featureless to make an unambiguous 1^+ spin-parity assignments, they are consistent with the predictions of a microscopic calculation in which a pure proton $(h_{11/2}^{-1} h_{9/2}^{1})_{1^+}$ excitation is assumed (the solid line in fig.5). If the observed states at 7.06 and 8.01 MeV are indeed 1^+ states then they exhaust 35% and 31% of the maximum proton 1p-1h excitation strength, respectively. A neutron contribution $(i_{13/2}^{-1} i_{11/2})$ due to the nuclear tensor force would not effect the shape of the calculated angular distribution.

In a recent electron scattering experiment [20] evidence for a strong M1 excitation at 7.20 MeV has been found. We observe a strong state at 7.24 MeV where a 1^- excitation has been suggested[21]. The angular distribution of this state is shown in fig.6 together with dipole states at 6.26, 6.72 and 7.08 MeV. As compared to the dipole states which are consistent with ref.2 the angular distribution of the 7.24 MeV state is better described by the microscopic M1 calculation. Its excitation strength would correspond to about 30% of the maximum M1 proton strength. A dipole state at this energy as found in ref.21 is not seen in the (γ,γ') reaction[22]. Therefore it should have a width much smaller than that of the 1^- state at 7.33 MeV (Which is strongly excited in (γ,γ')) and should also be weakly excited in (p,p').
It should be noted that a strong 1^+ state (at 7.28 MeV) has been found also in angular correlation studies of the (γ,γ') reaction[23], and also the energy dependence of a strong peak at 7.22 MeV seen in 180^o electron scattering [24] is consistent with M1. Thus, the existing data are consistent with a 1^+ assignment. However, three strong 1^+ states (at energies of about 7, 7.2 and 8 MeV) are not expected in simple models (see e.g. ref.25). Although

detailed calculations[26] show that the fine structure of the M1 excitation (which is critically dependent on the proton-neutron force) can exhibit a more complicated structure more experimental data are needed to clarify the problem of strong M1 excitations in ^{208}Pb.

New experimental evidence for collective M1 strength at around 7.5 and above 8 MeV has been reported in refs. 27 and 28. Such excitations have rather small widths and may be weakly excited in (p,p'). However, it is interesting to note that the energies of possible M1 excitations above 8 MeV in ref.27 coincide with the states which we identified as quadrupole states (see sect. IV.1). Estimates of ground state widths of the quadrupole excitations from our data are consistent with the electron scattering data of ref.18 and will be discussed elsewhere[5]. It would suggest that the positive parity states observed in ref.27 are in fact not 1^+ but 2^+ states.

IV.3. Dipole (L=1) Excitations and radiative widths from (p,p')

The most pronounced angular distributions in fig.2 are those of L=1 structure. They have a characteristic forward rise and can be distinguished easily from other transitions. Below the neutron threshold we observe pronounced dipole excitations at 6.26, 6.72 and 7.08 MeV, there angular distributions are shown in fig.6. The assumption of $J^\pi = 1^-$ for these states is consistent with results in refs. 2 and 22. In particular the 6.26 MeV state has been identified as a 1^- state in different experiments (see ref.29). However, in contrast to the fall off at large angles expected for isovector dipole it shows a large angle enhancement of the cross section. This is not found for the other dipole excitations at 6.72 and 7.08 MeV which for large angles clearly disappear under the background. As will be discussed below the large angle enhancement for the 6.26 MeV state can be explained by an isoscalar dipole (non-spin-flip) contribution indicated by the dot-dashed line in fig.6.

In the high energy region discussed in sect.IV.1. there are many dipole states seen in (γ,n)[19], some of them with large ground state widths. In our (p,p') experiment very little evidence for these dipole states is found. Only in the energy region around 8 MeV a group of strong states have been found which have the characteristic forward peaking of L=1 structure (see fig.7). It should be noted that, although the cross sections have large uncertainties due to subtraction of background and neighbouring structure, the spectra clearly indicate the strong forward rise typical for L=1. This group of states is excited in our experiment differently from γinduced reactions, e.g. is the 8.37 MeV state seen in the (γ,n) reaction[1,19,27] with a cross section more than one order of magnitude smaller than expected from our strong excitation (if an isovector dipole mode is assumed). This suggests a rather strong excitation of other than isovector dipole.

To make a more quantitative comparison with γ induced reactions we made an attempt to derive radiative widths from our inelastic strengths. Of course, in such an estimate enter uncertainties in the effective interaction and in the transition density. So is e.g. for dipole excitations the width larger for a surface peaked transition density as obtained from refs. 8 and 9 then for a density with radial node. In the inelastic form factor, however, the contribution from the nuclear interior is damped out by absorption. Thus, the comparison of (p,p') and γ induced reactions may be used to study the details of dipole transition densities. The ground state width (see ref.30) is given by

$$\Gamma_0(EL)[\text{eV}] = 1.44\cdot10^6 \frac{8\pi(L+1)}{L[(2L+1)!!]^2} (5.083\cdot10^{-3}\cdot E_x)^{(2L+1)} \langle r^L \rangle_c^2 \qquad (7)$$

where E_x is the excitation in MeV. $\langle r^L \rangle_c = \int \rho_{TR}^c(r) r^{L+2} dr$, this is related to the inelastic form factor by eq. (1) and (2).

If collective model transition densities (e.g. from refs. 8 and 9) are used then the experimental widths from γ induced reactions for 1^- excitations correspond to very small cross sections in proton scattering, e.g. in the high energy region the expected dipole excitation is generally more than five times weaker than our quadrupole excitations in fig.3. Even the strong excitation at about 9.40 MeV with a width of 26 eV[19] would yield a cross section in (p,p') less than 10 μb/sr at 10°.

The extracted ground state widths from our inelastic strengths are given in table 2. The fact that they are generally larger than the experimental width may be due to two effects:

a) the structure is isovector dipole but the transition density is rather different from that of the collective state,

b) the structure is different from isovector dipole.

As discussed above the first effect can lead to enhanced inelastic strengths for particular structures, e.g. single-particle structures with radial node in the transition density and could explain to some extend the larger proton widths in table 2. However, drastic differences between strengths extracted from inelastic and electromagnetic transitions are not expected because in both processes the contribution from the region close to the nuclear surface is largest. Therefore the observed strong enhancement of the dipole excitation for some should be connected with the second effect.

IV.4. Collective Dipole Spin-Flip (L=1, S=1) Excitations

The fact that two of our strong dipole excitations have a strength more than one order of magnitude larger than observed in γ induced reactions clearly indicates a structure different from isovector dipole. Possible L=1 excitations which yield retarded matrix elements in γ induced reactions are isoscalar dipole and dipole spin-flip (L=1, S=1) the latter can lead to final states of 0^-, 1^-, and 2^-. The dipole states with large isoscalar non-spin-flip

component should be excited in α scattering. This type of excitation can be described as a diffuseness oscillation and is discussed in detail in ref.31. We have measured the energy region in question in α scattering and a spectrum is shown in fig.8. At none of the measured angles between 10^{o} and 20^{o} were the states of interest found to be excited in contrast to states at lower excitation energy of 4.84, 5.28 and 5.50 MeV, where strong dipole excitations were observed. This rules out an isoscalar (non-spin-flip) assignment for the higher states. Only at 6.26 MeV an excitation is seen in α scattering which has a strength of about 10% of that found for the 5.50 MeV state. An isoscalar excitation is shown in fig.8 by the dot-dashed line (the details of this calculation together with a discussion of strong isoscalar dipole excitations at 4.84, 5.28 and 5.50 MeV are given elsewhere[31]). This type of excitation can explain the enhanced cross section at larger angles found for this state and reduces the derived width by about 35%. However, the strong discrepancy between inelastic excitation strength and measured width still exists.

We conclude that the observed dipole strength can be explained only by assuming a significant dipole spin-flip (L=1, S=1) component. It has to be noted that the energies of our peaks at 7.40 and 7.92 MeV coincide with those of two excitations recently found in large angle electron scattering[24] which have been identified as M2 excitations. At the energies of the other states 1^{-} states are known[1,2,19,22,27,29]. So our conclusions are consistent with the other available experimental results, suggesting the excitation of 1^{-} and 2^{-} states. For the two possible 2^{-} excitations the strengths obtained from the DWBA fits are given in table 3. For the transition density the radial form from the Goldhaber-Teller model[8] is used, this yields a good description of the angular distributions in fig.7. If the radial form is used from the Jensen-Steinwedel model[9] less structured angular distributions are obtained and the strength is increased by about 15%. Although for the extraction of B(M2)

values from p scattering similar uncertainties exist as for estimations of dipole widths (see sect.IV.3) our results in table 3 are in excellent agreement with the electron scattering results[24].

The other states at 6.26 and 8.37 may indicate collective 1^{-} spin-flip excitations. By using a surface peaked transition density as from the Goldhaber-Teller model, the DWBA calculations yield rather large sum rule strengths of 25 and 14% for the 6.26 and 8.37 MeV state, respectively. (assuming the sum rule strength the same as for the isovector dipole).

One may question if the structure of the strong 6.26 MeV state is not related to the isoscalar excitations around 5 MeV (ref.31). Its excitation strength is very close to that of the 5.5 MeV state, this may support an isoscalar spin-flip interpretation.

Our experimental evidence for strong dipole spin-flip excitations is supported by several theoretical studies. In the RPA calculations of refs.25 and 3 large M2 strength is predicted at 7.5 MeV. Further, in studies of 1^{-} excitations[33] a large isoscalar and isovector spin-flip strength is obtained in th energy region of 8-11 MeV, and in recent RPA calculations[34] collective 1^{-} spin-flip states have been found around 7.9 and 8.9 MeV.

Summary

Our high resolution proton scattering experiment has shown a pronounced structure in the high excitation region of ^{208}Pb. The region is different from the low excitation which has been studied by Wagner et al.[29] in that the excitation character changes rapidly with energy showing concentrations of states with the same multipolarities. This indicates strong collective excitations. We observe many quadrupole states above 8.5 MeV in the region of the giant quadrupole resonance (centered around 10.5 MeV). At lower energies between 6 and 8.5 MeV we observe a concentration of dipole (L=1) excitations.

The excitations at 7.40 and 7.92 MeV are described consistent with results from 180° electron scattering and suggest a collective 2^- excitation. The strong states at 6.26 and 8.37 MeV yield evidence for a collective 1^- spin-flip excitation. The fact that 1^- and 2^- spin-flip structures have been found between 6 and 8 MeV may indicate a concentration of the spin-flip strength in this excitation region. That no large enhancement of the cross section is observed is only due to the nature of the nucleon-nucleon force which yields (assuming Serber force) one order of magnitude smaller cross sections for the spin-flip excitation as compared to the isoscalar non-spin-flip excitation. Further studies should be performed to see if these spin-flip excitations are found for other nuclei and to see if they represent a general property of nuclear excitations.

The authors are indebted to G.F.Bertsch for valuable discussion.

This work has been supported by the National Science Foundation.

References

1. R.J.Holt and H.E.Jackson, Phys.Rev.Lett.36(1976)244 and R.J.Holt, R.M.Laszewski and H.E.Jackson, Phys.Rev.C15(1977)827.
2. S.J.Freedman et al., Phys.Rev.Lett.37(1976)1606.
3. R.G.Markham and R.G.H.Robertson, Nucl.Instr. and Meth. 129(1975)263.
4. H.P.Morsch, P.Decowski and W.Benenson, Phys.Rev.Lett.37(1976)263.
5. H.P.Morsch, P.Decowski and W.Beneson, to be published.
6. I.Reichstein and Y.C.Tang, Nucl.Phys.A139(1969)144.
7. S.M.Austin in "The Two-Body Force in Nuclei", edited by S.M.Austin and G.M.Crawley (Plenum, New York-London,1972),p.285, and references therein.
8. M.Goldhaber and E.Teller, Phys.Rev.74(1948)1046.
9. H.Steinwedel, J.H.D.Jensen and P.Jensen, Phys.Rev.79(1950)1019.
10. F.D.Becchetti and G.W.Greenlees, Phys.Rev.182(1969)1190.
11. G.R.Satchler, Nucl.Phys.77(1966)481.
12. A.M.Lane, Nuclear Theory (Benjamin, New York)1965.
13. F.E.Bertrand, D.C.Kocher, Phys.Rev.C13(1976)2241.
14. F.R.Buskirk et al., Phys.Lett.42B(1972)194.
15. M.Nagao and Y.Torizuka, Phys.Rev.Lett.30(1973)1068.
16. M.N.Harakeh et al., Phys.Rev.Lett.38(1977)676.
17. R.Pitthan et al., Phys.Rev.Lett.33(1974)849.
18. A.Schwierczinski et al., Phys.Rev.Lett.35(1975)1244.
19. N.K.Sherman et al., Phys.Rev.Lett.35(1975)1215.
20. R.Frey et al., to be published, and A.Richter and W.Knüpfer, private communication.
21. E.D.Earle et al., Phys.Lett.32B(1970)471.
22. G.A.Bartholomew et al., Adv. in Nucl.Phys. 7(1973)229.
23. A.Wolf et al., Phys.Rev.C6(1972)2276.
24. R.A.Lindgren et al., Phys.Rev.Lett.35(1975)1423.

References (continued)

25. P.Ring and J.Speth, Nucl.Phys.A235(1974)315.

26. J.S.Dehesa, J.Speth and A.Faessler, Phys.Rev.Lett.38(1977)208.

27. R.H.Laszewsky, R.J.Holt and H.E.Jackson, Phys.Rev.Lett.38(1977)813.

28. D.J.Horen, J.A.Harvey and N.W.Hill, Phys.Rev.Lett.38(1977)1344.

29. W.T.Wagner et al., Phys.Rev.C12(1975)757.

30. A.Bohr and B.R.Mottelson, Nuclear Structure, Vol.I (Benjamin, New York).

31. P.Decowski, H.P.Morsch and W.Benenson, to be published.

32. E.Grecksch, W.Knüpfer and M.G.Huber, Lett.Nuovo Cim.14(1975)505.

33. M.Harvey and F.C.Khanna, Nucl.Phys.A221(1974)77.

34. J.Speth, private communication.

Figure Captions

1. Spectrum of protons at 15° from the reaction ^{208}Pb(p,p') at 45 MeV. The solid line represents an assumed smooth background originating from compound and precompound processes as well as direct processes exciting many overlapping levels in this high level density region. The dashed line represents a local background assumed for extraction of the intensity of the stronger states. The horisontal line mark observed structures at 9.3, 10.1, and 11.1 MeV.

2. Differential cross sections of transitions with various multipolarities exhausting 100% of energy weighted sum rule at an excitation energy of 10 MeV (for L=0,2,3 isoscalar, for L=1, S=0 isovector).

3. Angular distributions of narrow peaks observed in the giant resonance region of ^{208}Pb. The solid lines represent calculations for L=2 and 3 isoscalar excitation.

4. Angular distributions of gross structures observed in the giant resonance region of ^{208}Pb. For the 9.3 MeV peak the curves represent isoscalar excitation, whereas lines for the 10.1 and 11.1 MeV structures correspond to calculations including small isovector contributions as discussed in the text.

5. Angular distributions for states at 7.06 and 8.01 MeV excited in proton scattering. The solid lines represent microscopic DWBA calculations assuming a magnetic dipole (1^+) excitation.

6. Angular distributions for states at 7.24 MeV; 6.26, 6.72 and 7.08 MeV. For the 7.24 MeV state the solid line corresponds to a microscopic calculation assuming a M1 excitation. The lines for the other states (dashed for the 6.26 MeV and solid for the 6.72 and 7.08 MeV states) correspond to calculations assuming an isovector dipole excitation.

7. Angular distributions of dipole states observed in the excitation region 7-8.5 Me

8. Spectrum of α particles from the ^{208}Pb(α,α') reaction at 48 MeV and 14°.

Table 1: Percent of the energy weighted sum rule in the observed transitions in the high excitation region of ^{208}Pb.

L=2,S=0,ΔT=0		L=3,S=0,ΔT=0	
E_x MeV	% of EWSR	E_x MeV	% of EWSR
8.62	1.6	8.16	2.4
8.75	1.8	8.47	1.0
8.95	1.4	8.83	0.8
9.31	1.7	9.18	1.1
9.52	2.1	9.38	1.3
Total	8.6	Total	6.6
Gross Structure at 9.3	5.2	Gross Structure at 9.3	13.0

Table 2 : Comparison of ground state radiative widths deduced from our inelastic strength (assuming 1^- excitation) with experimental widths from γ induced reactions (refs. 1,2,19,22,27).

E_x MeV	J^π	Γ_0[eV] from (p,p')	exp[a]	$[\Gamma_0(p,p')/\Gamma_0(exp)]^{\frac{1}{2}}$ (1^-)
6.26	1^-	138	4	5.9
6.72	1^-	72	14.5	2.2
7.08	1^-	54	12	2.1
7.33	1^-	71[c]	50	1.2
7.40	2^- [b]	27	small	
7.92	$1^-,2^-$ [b]	58	13	
8.22	1^-	16	10	1.3
8.37	1^-	71	3.5-6	.4
9.38	1^-	60[c]	26	1.5

a) from refs. 1,2,19,22,27

b) 2^- assignment from ref.24.

c) estimated from forward angle cross sections.

Table 3 : Comparison of B(M2) values deduced from our inelastic strength (assuming 2^- excitation) with experimental results from ref.24.

E_x MeV	J^π	B(M2)[$\mu_0^2 fm^2$] from (p,p')	(e,e')[a]
7.40	2^-	450	449
7.92	2^-	727	614

a) from ref.24.

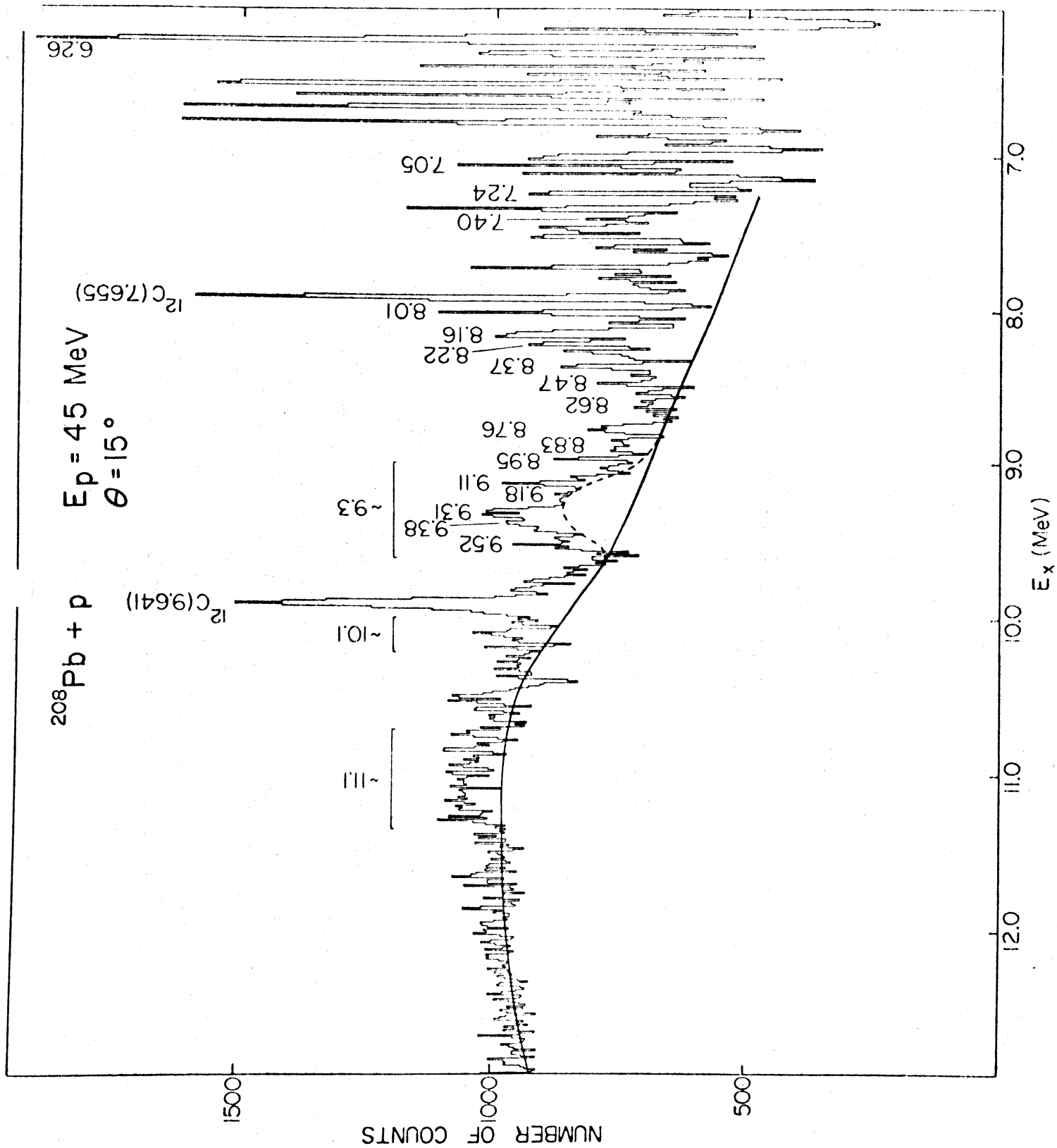
^{208}Pb + p
E_p = 45 MeV
θ = 15°
^{12}C(9.641)
^{12}C(7.655)
~11.1
~10.1
~9.3
9.52
9.38
9.31
9.18
9.11
8.95
8.83
8.76
8.62
8.47
8.37
8.22
8.16
8.01
7.40
7.24
7.05
6.26
NUMBER OF COUNTS
1500
1000
500
12.0
11.0
10.0
9.0
8.0
7.0
E_x (MeV)

Fig. 1.

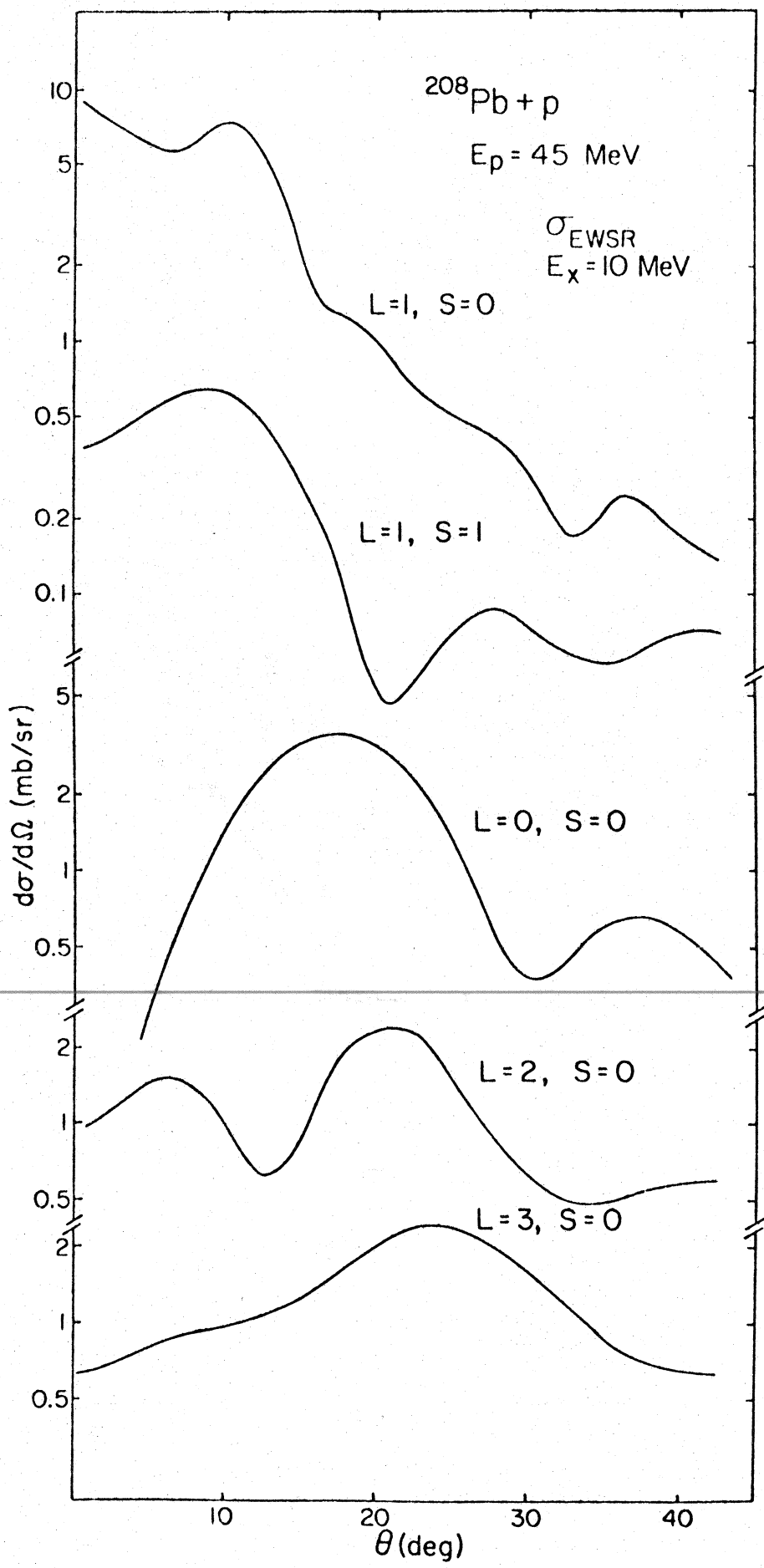
^{208}Pb + p
E_p = 45 MeV
σ_{EWSR}
E_x = 10 MeV
L=1, S=0
L=1, S=1
L=0, S=0
L=2, S=0
L=3, S=0
dσ/dΩ (mb/sr)
θ (deg)

Fig. 2.

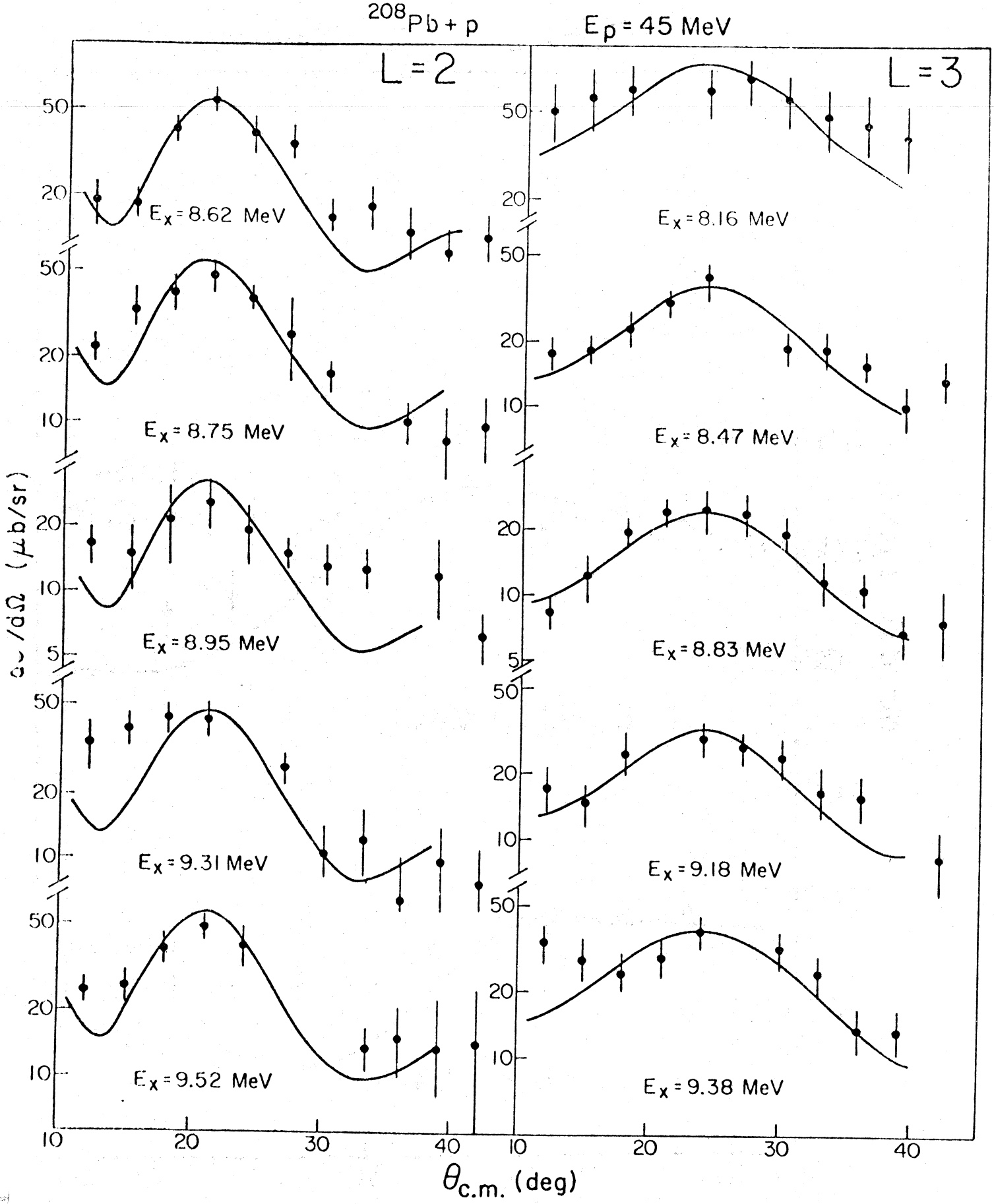
^{208}Pb + p
E_p = 45 MeV
L = 2
L = 3
E_x = 8.62 MeV
E_x = 8.16 MeV
E_x = 8.75 MeV
E_x = 8.47 MeV
E_x = 8.95 MeV
E_x = 8.83 MeV
E_x = 9.31 MeV
E_x = 9.18 MeV
E_x = 9.52 MeV
E_x = 9.38 MeV
dσ/dΩ (μb/sr)
$\theta_{c.m.}$ (deg)

Fig. 3.

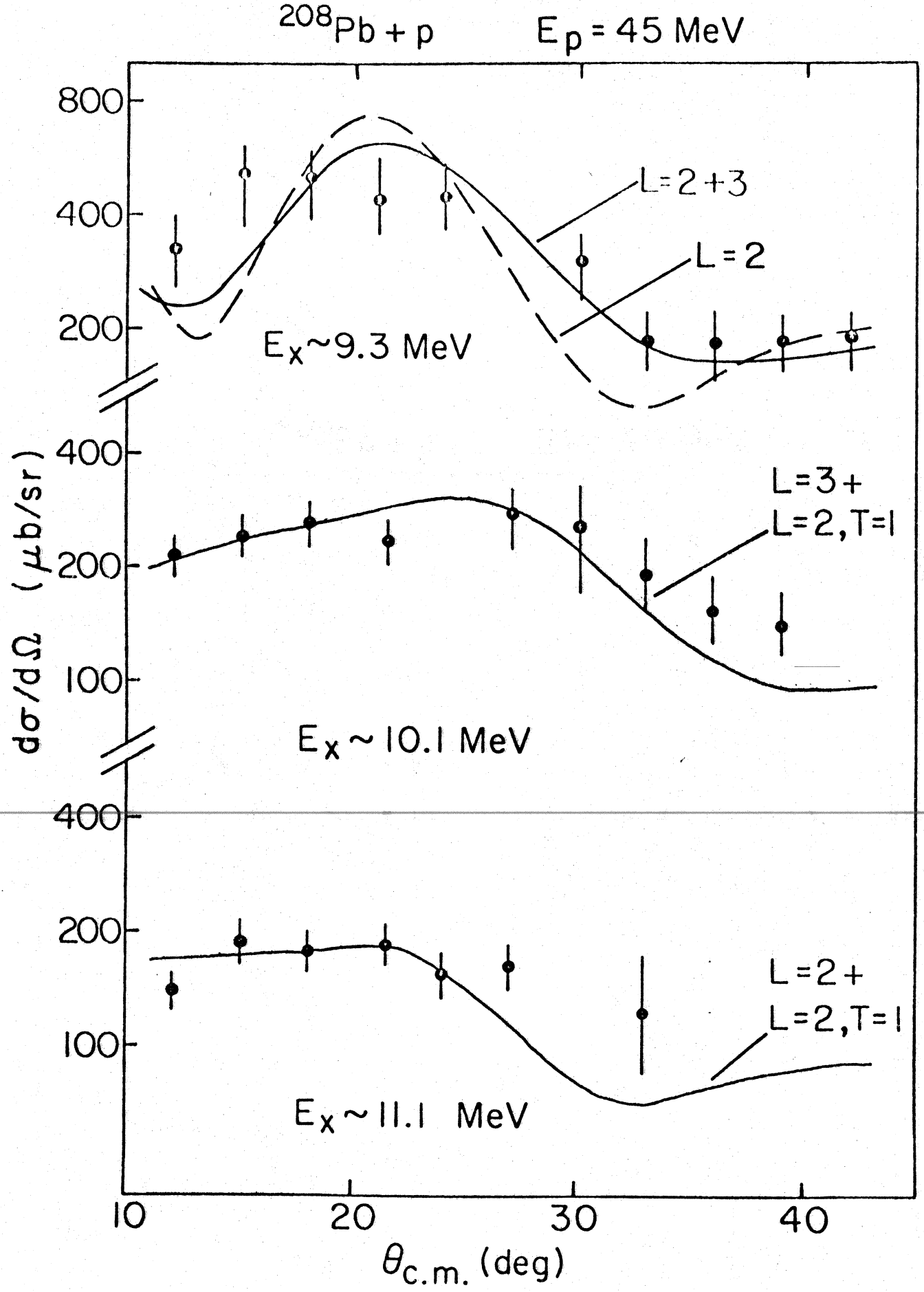
^{208}Pb + p
E_p = 45 MeV
800
400
200
L=2+3
L=2
E_x~9.3 MeV
400
200
100
L=3+
L=2,T=1
E_x ~ 10.1 MeV
400
200
100
L=2+
L=2,T=1
E_x ~ 11.1 MeV
dσ/dΩ (μb/sr)
10
20
30
40
$\theta_{c.m.}$ (deg)

Fig. 4.

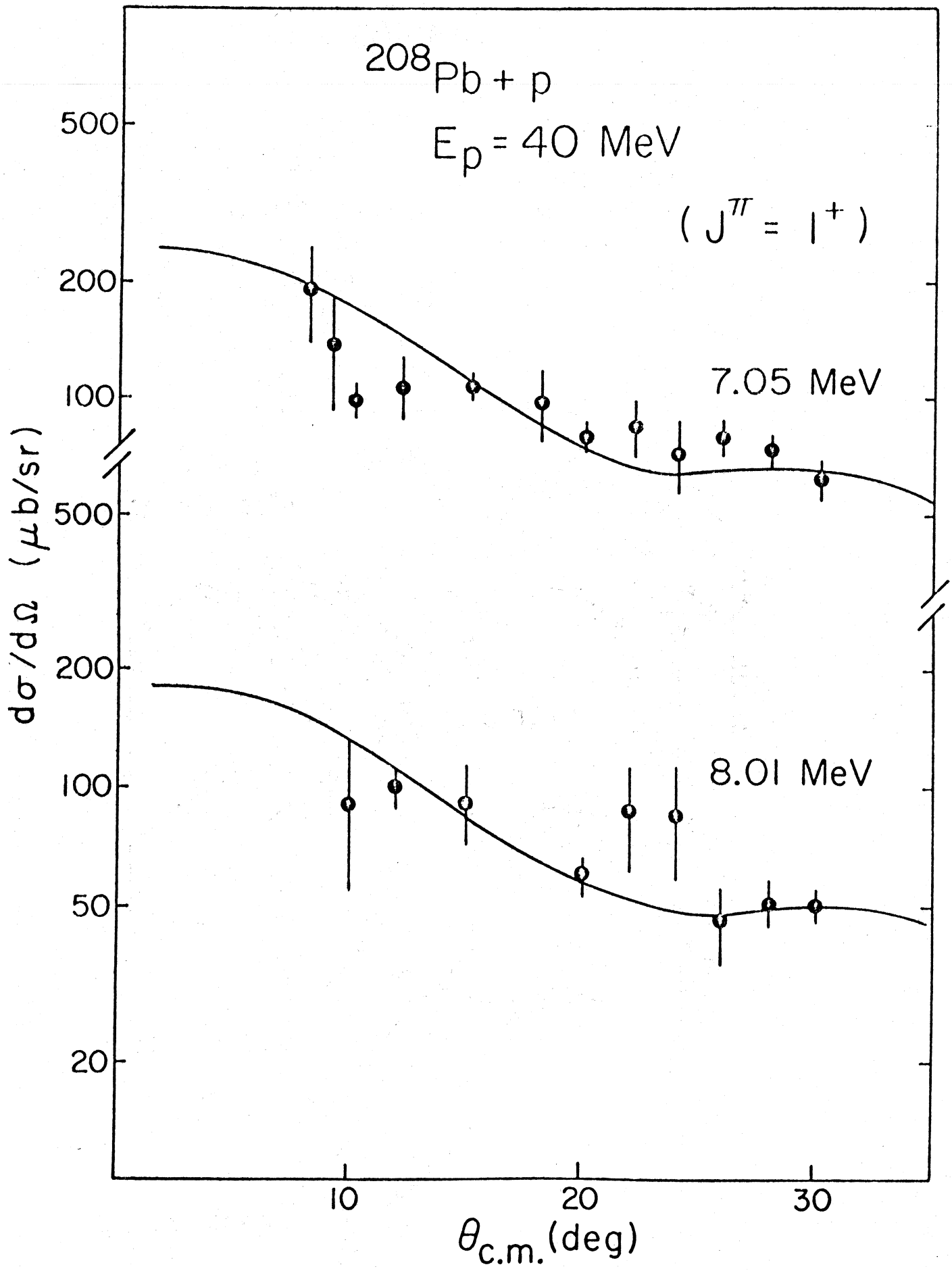
^{208}Pb + p
E_p = 40 MeV
(J^{π} = 1^+)
7.05 MeV
8.01 MeV
dσ/dΩ (μb/sr)
500
200
100
50
20
10
20
30
$\theta_{c.m.}$ (deg)

Fig. 5.

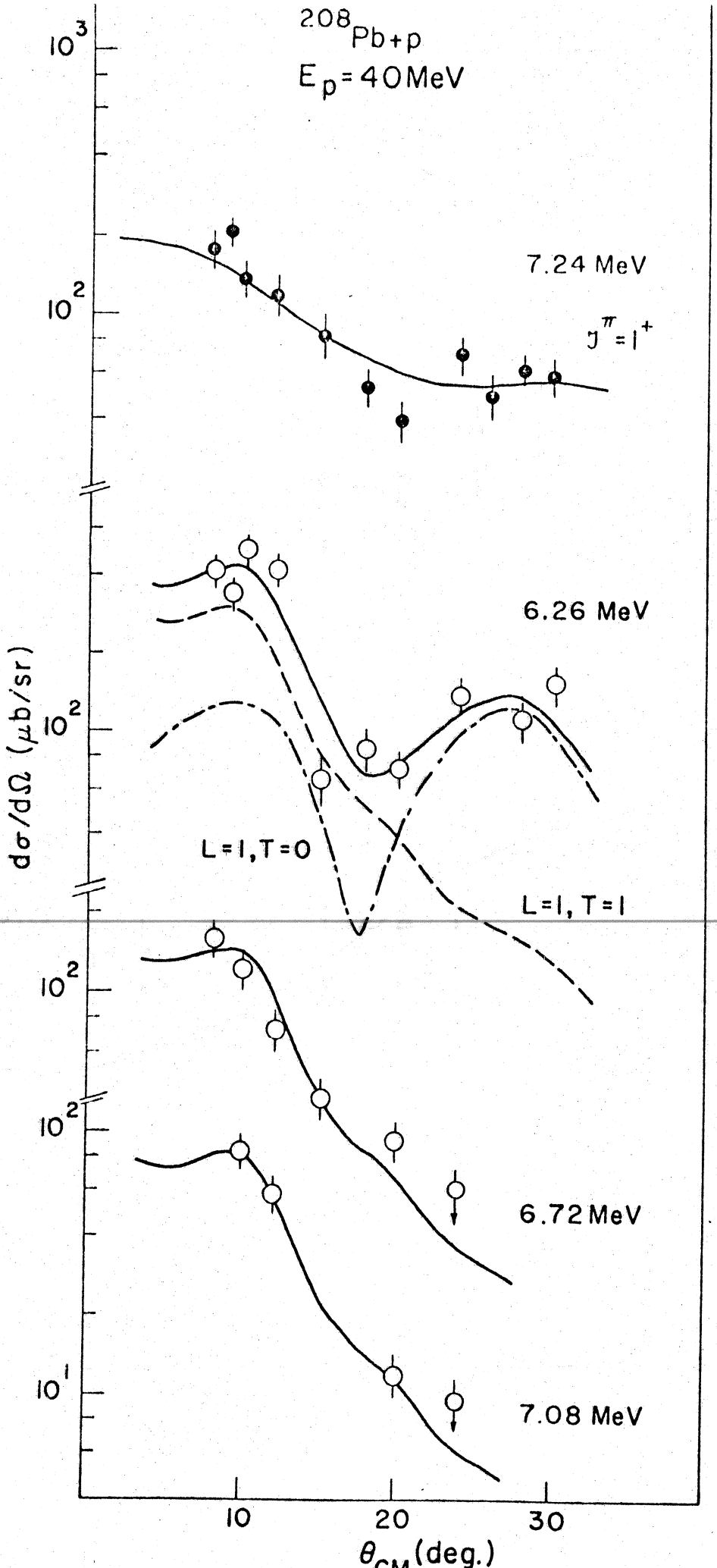
^{208}Pb+p
E_p = 40 MeV
7.24 MeV
$J^\pi = 1^+$
6.26 MeV
L=1, T=0
L=1, T=1
6.72 MeV
7.08 MeV
$d\sigma/d\Omega$ (μb/sr)
10^3
10^2
10^2
10^2
10^1
10
20
30
θ_{CM} (deg.)

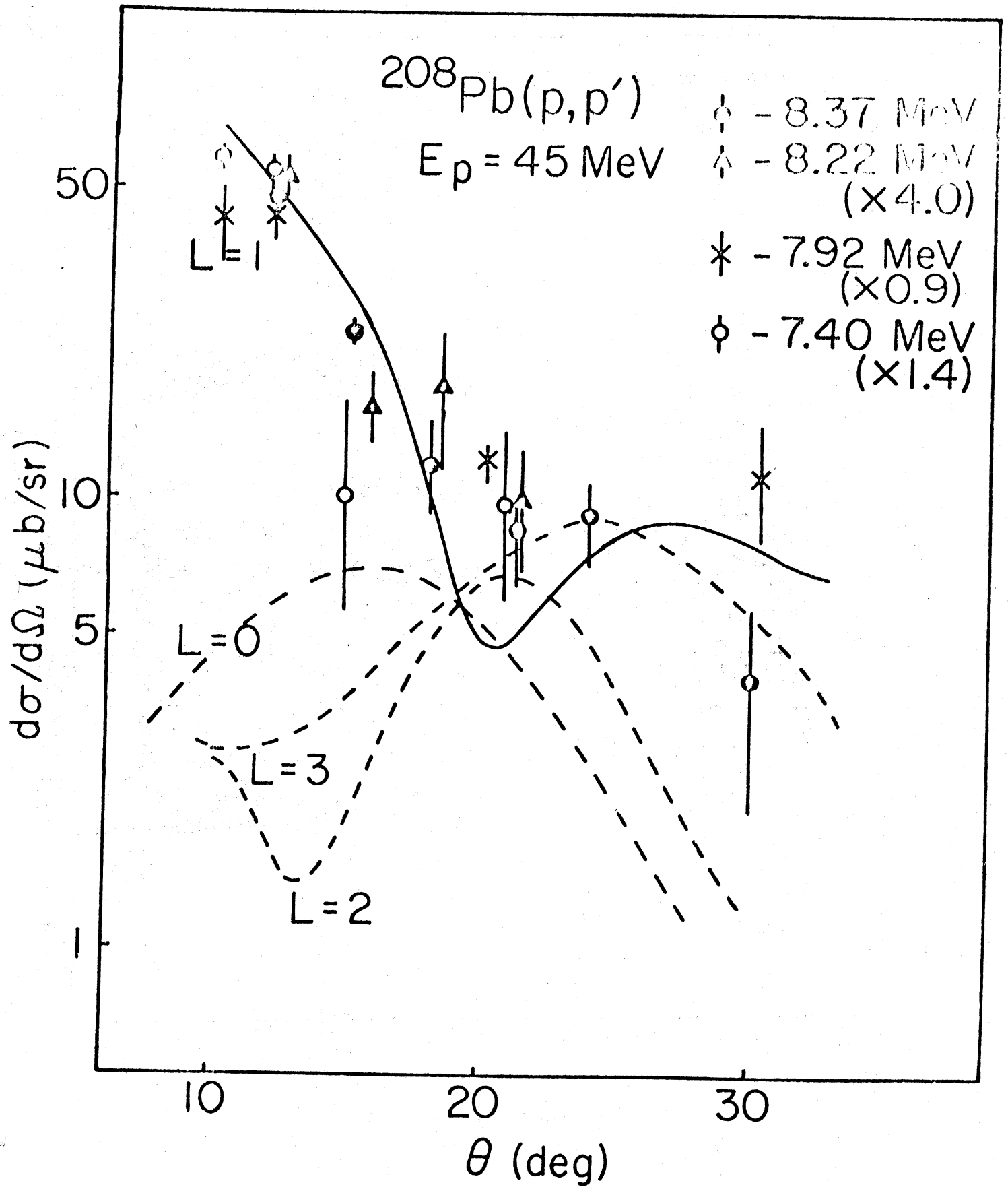
^{208}Pb(p,p′)
E_p = 45 MeV
8.37 MeV
8.22 MeV (×4.0)
7.92 MeV (×0.9)
7.40 MeV (×1.4)
L=1
L=6
L=3
L=2
50
10
5
1
dσ/dΩ (μb/sr)
10
20
30
θ (deg)

Fig. 7.

Fig. 8.

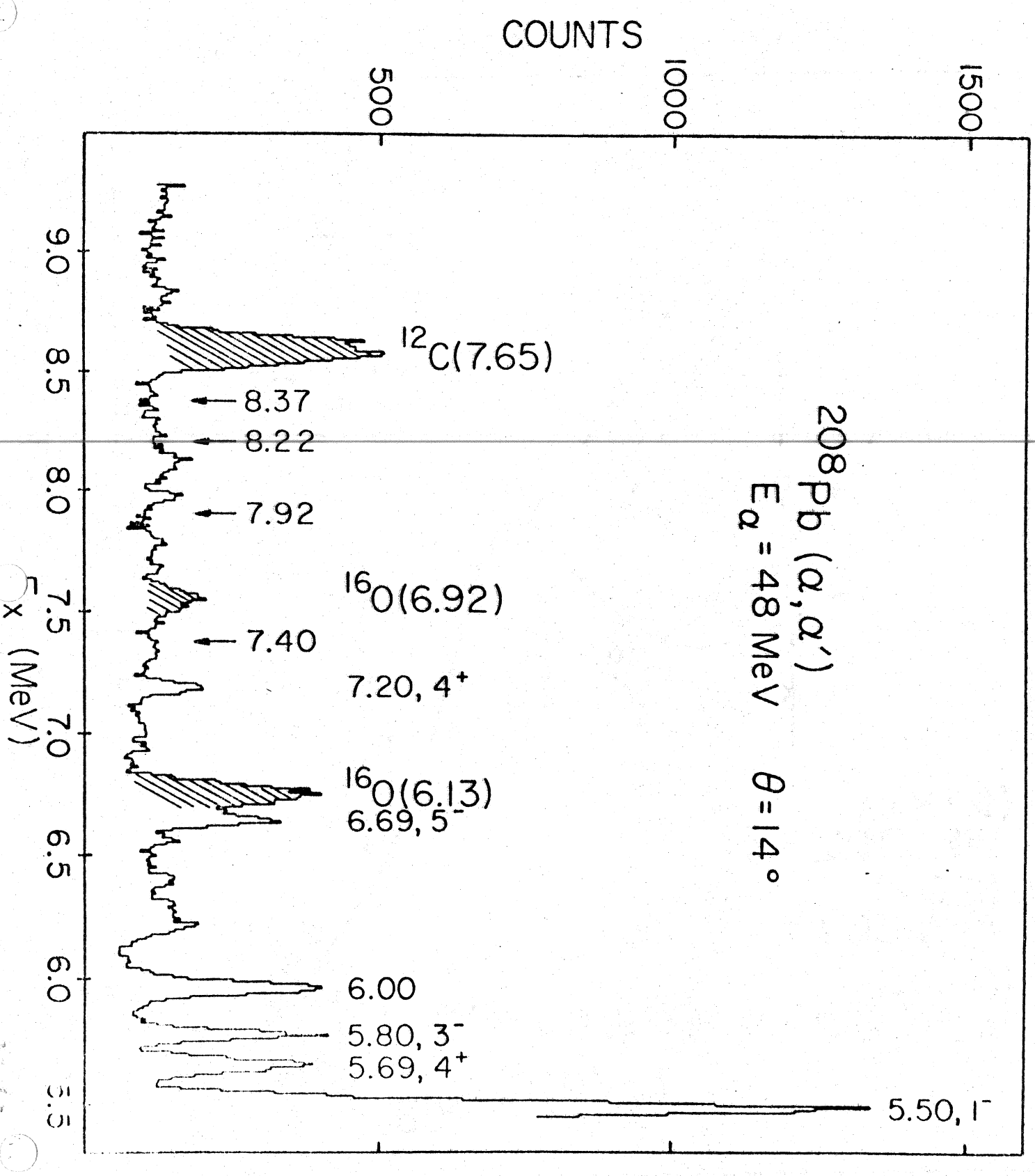
COUNTS
500
1000
1500
9.0
8.5
8.0
7.5
7.0
6.5
6.0
5.5
E_x (MeV)
^{208}Pb (α,α')
E_α = 48 MeV
θ = 14°
^{12}C(7.65)
8.37
8.22
7.92
^{16}O(6.92)
7.40
7.20, 4$^+$
^{16}O(6.13)
6.69, 5$^-$
6.00
5.80, 3$^-$
5.69, 4$^+$
5.50, 1$^-$